Cerebral Cortex November 2010;20:2728–2738
doi:10.1093/cercor/bhq019
Advance Access publication February 26, 2010

The Ventral and Inferolateral Aspects of the Anterior Temporal Lobe Are Crucial in Semantic Memory: Evidence from a Novel Direct Comparison of Distortion-Corrected fMRI, rTMS, and Semantic Dementia

Richard J. Binney[1], Karl V. Embleton[1,2], Elizabeth Jefferies[3], Geoffrey J. M. Parker[2] and Matthew A. Lambon Ralph[1]

[1]Neuroscience and Aphasia Research Unit, School of Psychological Sciences, University of Manchester, Manchester, M13 9PL, UK, [2]Imaging Sciences Research Group, Research School of Cancer and Imaging Sciences, School of Medicine, University of Manchester, Manchester, M13 9PT, UK and [3]Department of Psychology, University of York, York YO10 5DD, UK

Address correspondence to Prof. Matthew A. Lambon Ralph, Neuroscience and Aphasia Research Unit, Zochonis Building, School of Psychological Sciences, University of Manchester, Oxford Road, Manchester M13 9PL, UK. Email: matt.lambon-ralph@manchester.ac.uk.

Although there is an emerging consensus that the anterior temporal lobes (ATLs) are involved in semantic memory, it is currently unclear which specific parts of this region are implicated in semantic representation. Answers to this question are difficult to glean from the existing literature for 3 reasons: 1) lesions of relevant patient groups tend to encompass the whole ATL region; 2) while local effects of repetitive transcranial magnetic stimulation (rTMS) are spatially more specific, only the lateral aspects of the ATL are available to stimulation; and 3) until recently, functional magnetic resonance imaging (fMRI) studies were hindered by technical limitations such as signal distortion and dropout due to magnetic inhomogeneities and also, in some cases, by methodological factors, including a restricted field of view and the choice of baseline contrast for subtraction analysis. By utilizing the same semantic task across semantic dementia, rTMS, and distortion-corrected fMRI in normal participants, we directly compared the results across the 3 methods for the first time. The findings were highly convergent and indicated that crucial regions within the ATL for semantic representation include the anterior inferior temporal gyrus, anterior fusiform gyrus, and the anterior superior temporal sulcus.

Keywords: anterior temporal lobes, functional magnetic resonance imaging, repetitive transcranial magnetic stimulation, semantic cognition, semantic dementia

Introduction

Semantic cognition refers to a collection of higher cortical functions that permit us to encode and use the meaning of words and objects in order to generate flexible and sophisticated verbal and nonverbal behavior (Rogers and McClelland 2004; Jefferies and Lambon Ralph 2006). Although it was an issue of considerable debate (e.g., Martin 2007), there is now a growing consensus that the (bilateral) anterior temporal lobe (ATL) plays an important role in semantic memory (Patterson et al. 2007; Lambon Ralph and Patterson 2008; Simmons and Martin 2009). The longest standing and richest evidence stems from patients with semantic dementia (SD), who exhibit a progressive yet highly selective impairment of semantic memory whilst other aspects of perception and cognition function are largely unaffected (Hodges et al. 1992). Semantic performance is impaired in receptive and expressive tasks across all modalities, including spoken and written words, pictures, environmental sounds, smell, touch, and taste (Lambon Ralph et al. 1999, 2001; Bozeat et al. 2000, 2002, 2003; Coccia et al. 2004; Luzzi et al. 2007; Piwnica-Worms et al. forthcoming). This striking behavioral profile is coupled with relatively circumscribed atrophy and hypometabolism of the bilateral ATLs. The pairing of a selective pan-modal semantic impairment with ATL atrophy has led to the suggestion that this region (bilaterally) is critical in the formation of amodal conceptual representations (Rogers et al. 2004; Patterson et al. 2007; Lambon Ralph and Patterson 2008; Lambon Ralph et al. forthcoming).

Some forms of neuroimaging also implicate a role for the ATL in semantic processing (Binder et al. 2009; Visser et al. forthcoming)—including positron emission tomography (PET) (Vandenberghe et al. 1996; Scott et al. 2000; Crinion et al. 2003; Rogers et al. 2006; Spitsyna et al. 2006) and magnetoencephalography (MEG) (e.g., Marinkovic et al. 2003). Furthermore, repetitive transcranial magnetic stimulation (rTMS) to the lateral ATL selectively slows performance in receptive (synonym judgment) and expressive (picture-naming) semantic tasks but has no effect on nonsemantic (number-based) tests matched for overall difficulty (Pobric et al. 2007). This pattern holds whether left or right temporal poles are stimulated (Lambon Ralph et al. 2009).

Convergent evidence from functional neuroimaging and transcranial magnetic stimulation (TMS) is important for 2 reasons. First, because SD is underpinned by a neurodegenerative disease, there is a possibility that subthreshold damage or dysfunction due to spreading pathology contributes to the patients' semantic impairment (Hickok and Poeppel 2004; Martin 2007). The second motivation for convergent evidence, especially from functional magnetic resonance imaging (fMRI) in neurologically intact participants, concerns our ability to answer a new set of research questions that have arisen from the recent inclusion of the ATL in models of semantic cognition: 1) Which specific regions within the ATL contribute to semantic memory and 2) what role or type of information do they add (Lambon Ralph and Patterson 2008; Simmons and Martin 2009; Lambon Ralph et al. forthcoming)? The first of these new research questions is the target of the present study.

At present, even the simple definition of what constitutes the ATL is somewhat unclear. Many authors, including ourselves, have used the term "ATL" to simply refer to those regions primarily affected in SD (e.g., Patterson et al. 2007). This lacks specificity, given that, on the basis of relevant volumetric and metabolic studies (Mummery et al. 2000; Galton et al. 2001; Nestor et al. 2006), SD implicates a rather broad region incorporating a large proportion of the rostral half of the temporal lobe (see Fig. 1*e*). Moreover, it might be inferred from the theories and computational models predicated on SD

studies (e.g., Rogers et al. 2004; Patterson et al. 2007) that the ATL is a functionally homogenous structure. It has yet to become apparent, however, whether the semantic function ascribed to it really requires this entire area. Neuroanatomically speaking, the prospect of this ATL region existing as a single unified functional entity seems unlikely. In considering the area typically affected in SD, it is possible to identify at least 8 cytoarchitecturally distinguishable albeit graded subregions (Brodmann 1909). In fact, it has been shown more recently that, in the temporopolar cortex alone, there is a minimum of 7 distinct subareas (Ding et al. 2009). Nonhuman primate studies also suggest that these subareas display differential patterns of connectivity to other cortical and subcortical regions (Morán et al. 1987; Gloor 1997). The primary goal of this study was, therefore, to determine which of these subregions are the most important for performing a semantic task and thus increase the anatomical specificity of hypotheses regarding anterior temporal involvement in conceptual processing.

The use of fMRI will be critical to achieving this goal, not only due to its superior spatial resolution as compared with other neuroimaging techniques such as PET and MEG, but also because there are limits in the extent to which SD studies and TMS can be used to probe differential function within the ATL. SD is a neurodegenerative disease, and as such, there is a graded distribution of tissue loss across the affected region rather than the absolute boundary found in acute stroke, for example. Volumetric studies of SD-related atrophy have shown that some ATL structures are more severely atrophied than others, and this might give some partial clues as to which subregions are the most important. Clearly though, SD studies are unlikely to dissociate different functions across different ATL subregions, given that all are affected in this disorder to some degree. Therefore, other techniques are required. The local effects of rTMS are much more spatially specific than brain disease, and indeed, this technique has been used in visual or motor-related regions to map out cortical receptive fields (Levy et al. 1991; Hamdy et al. 1996; Krings et al. 1998; Fernandez et al. 2002). While we have used this technique to probe the contribution of lateral ATL (at the anterior middle temporal gyrus [MTG]) to semantic processing (see above and Fig. 1*e,f*), it is anatomically impossible to map out the inferior surface or polar cap of the temporal lobes using TMS. It is important, however, to be able to probe the anterior inferior surface, given that 1) intracranial recordings suggest that these regions show relatively early and semantically selective neural activity (Liu et al. 2009), 2) a number of PET functional imaging studies find language-related activations in this region (Nobre et al. 1994; Vandenberghe et al. 1996; Devlin et al. 2000; Noppeney and Price 2002; Crinion et al. 2003; Sharp et al. 2004; Spitsyna et al. 2006), and 3) SD atrophy is particularly pronounced in this area (Chan et al. 2001; Galton et al. 2001; Studholme et al. 2004; Desgranges et al. 2007). So despite their limitations, by directly comparing results of previous rTMS studies and volumetric studies of SD with findings from an fMRI investigation, it may be possible to obtain valuable convergent evidence regarding ATL semantic function. This was the second aim of this study and was made possible through deliberate design choices that will be elaborated upon in the final section of this Introduction.

It is important to note, however, that until recently, fMRI and other neuroimaging studies have been somewhat silent over the involvement of the ATL in semantic memory. A formal meta-analysis showed that at least some of this absence of evidence reflects technical or methodological issues (Visser et al. forthcoming). These include imaging modality (PET is more likely to observe ATL activations than fMRI), field of view (a surprisingly large proportion of studies used a restricted field of view, which may have critically limited temporal lobe coverage in the respective analyses), and choice of baseline (low level, "rest" baselines were less likely to be associated with ATL activation). The difference between fMRI and PET almost certainly reflects the fact that the sensitivity of fMRI is not constant across the brain. The ATL and adjacent orbitofrontal cortex reside near air–bone interfaces that cause inhomogeneities in the magnetic field, leading to geometric image distortion and signal loss when using conventional gradient-echo echo planar imaging (EPI) (GE-EPI: Devlin et al. 2000; Dong et al. 2005; Blacker et al. 2006; Weiskopf et al. 2006). Recent improvements in engineering (e.g., parallel receiver coils) and image acquisition processing techniques (postacquisition k-space spatial-correction of spin-echo EPI [SE-EPI] data) have now reduced the problems associated with imaging the anterior inferior temporal lobes (Morgan et al. 2004; Embleton et al. forthcoming; Visser et al. in preparation), allowing us to adopt this successful ATL imaging "recipe" to tackle the core functional anatomy question underlying this study.

As alluded to above, our approach with this improved imaging method contained 2 elements. The first was simply to use the relatively good spatial resolution of fMRI, via standard whole-brain analysis, to investigate which subregions within the ATL are activated by a semantic task. Second, the study was deliberately designed in such a way to promote direct comparison and convergence with our previous neuropsychological and rTMS investigations of ATL semantic function. The validity of cross-referencing between experiments/methodologies with different activities is limited by discrepancies in the task requirements and stimuli employed. This means that, where differences arise between studies, it is unclear if they are true cross-methodology variations or simply reflect task/stimuli-specific differences. In a novel approach, therefore, we used a task and a set of stimuli for which we had already collected data from SD patients (Jefferies et al. 2009) and from normal healthy individuals taking part in ATL rTMS studies (Pobric et al. 2007; Lambon Ralph et al. 2009). Comparability was also improved by utilizing the same reaction-time matched nonsemantic control tasks from our rTMS experiments as a functional baseline for the fMRI study. By performing a set of planned region of interest (ROI) analyses (derived from measures of atrophy in SD and the site of rTMS stimulation) on the fMRI data, we directly assessed the commonality of semantic function highlighted by all 3 investigative techniques.

Methods

Participants

Fourteen healthy participants (9 males; age range = 19–36 years, mean age = 22.1, standard deviation = 4.8) took part in the experiment. All participants were native English speakers and right-handed, yielding a laterality quotient of at least 80 on the Edinburgh Handedness Inventory (Oldfield 1971). All had normal or corrected-to-normal vision. The experiments were reviewed and approved by the local ethics board.

Experimental Procedure

A PC running E-Prime software (Psychology Software Tools) was used for the presentation of stimuli. A block design was used. The

experiment consisted of ninety-six 20-s blocks. These blocks included 24 blocks of semantic judgment trials, 24 blocks of number judgment trials, and 48 blocks of rest (r), ordered in an r–A–r–B design. Within each semantic and number judgment block, there were 4 trials. Each trial lasted 5000 ms, comprising a fixation-cross presented for 1000 ms, followed by the stimuli that were presented for a fixed duration of 4000 ms in a black lowercase font on a white background. The participants were asked to respond to the stimuli by pressing 1 of 3 designated buttons on an magnetic resonance compatible response box.

As noted above, the semantic judgment task was the same as the one that we have developed to test comprehension in SD and other aphasic patient groups (Jefferies et al. 2009) and in our ATL rTMS experiments (Pobric et al. 2007; Lambon Ralph et al. 2009). In this task, the participant was asked to choose which of 3 choice words was most related to a probe word. Accordingly, each trial contained 4 written words: a probe word (e.g., ROGUE), the target choice (e.g., SCOUNDREL), and 2 unrelated choices (e.g., POLKA and GASKET). The 4 words within each trial were matched for imageability and word frequency (see Jefferies et al. 2009). The number judgment task (again extracted from our previous ATL rTMS studies) had the same format as the synonym judgment task: a probe number was presented at the top of the screen, and underneath, 3 number choices were provided. Participants were required to pick which of the 3 was closest in value. In the rTMS studies, we found that, by using double-digit numbers, the resultant number judgment times were typically slightly slower and less accurate than the synonym judgment tasks (see non-TMS data in Fig. 1*f*). Accordingly, any activation observed for the semantic task when directly contrasted against that of the control task could not be due to task difficulty. The rest blocks consisted of a 20-s continuous presentation of 4 fixation points that were displayed in a configuration that resembled the semantic and numerical tasks.

Imaging Acquisition

All imaging was performed on a 3T Philips Achieva scanner using an 8-element SENSE head coil with a sense factor of 2.5. The SE-EPI fMRI sequence included 42 slices covering the whole brain with echo time (TE) = 70 ms, time to repetition (TR) = 4150 ms, flip angle = 90°, 96 × 96 matrix, reconstructed resolution 2.5 × 2.5 mm, and slice thickness 3.0 mm. Brief (10 volumes for each k-space traversal) dual direction k-space traversal SE-EPI scans with matching parameters were conducted before the functional acquisitions in order to achieve sets of images matching the functional time series but with opposing direction distortions. These prescans were taken for each participant and were used to compute a spatial remapping matrix that could be applied to the functional time series (see below). The main fMRI image sequences of 465 time points were acquired with a single direction k-space traversal. A high-resolution T2-weighted turbo spin-echo scan with in-plane resolution of 0.94 mm and slice thickness 2.1 mm was also obtained as a structural reference to provide a qualitative indication of distortion correction accuracy.

Distortion Correction

The spatial remapping correction was computed using the method reported elsewhere (Embleton et al. forthcoming; Visser et al. in preparation). Briefly, in the first step, each volume of the main functional time series was registered to the original distorted mean prescan volume using a 12-degrees of freedom affine registration algorithm (FLIRT, FSL). Then for the correction step, a spatial transformation matrix was calculated from the opposingly distorted prescan images and then applied to the 465 time points in the functional acquisition. This resulted in a distortion-corrected data set of 465 volumes, maintaining the original temporal spacing and TR of 4150 ms.

fMRI Data Analysis

Analysis was carried out using statistical parametric mapping (SPM5) software (Wellcome Trust Centre for Neuroimaging). Single-subject functional EPI volumes were corrected for minor motion artifacts by registering to the first image volume using a rigid body spatial transform estimated using a least squares approach and second-degree B-spline interpolation. Subsequently, slice-timing correction referenced to the middle slice was performed using SPM5's Fourier phase shift interpolation. Functional image volumes were then transformed into standard stereotaxic space, according to the Montreal Neurological Institute (MNI) protocol, for intersubject averaging. This was achieved by estimating a 12-parameter affine transform and a nonlinear discrete cosine transform to register the mean EPI volume (obtained from realignment) to SPM5's EPI template and applying this transform to each image volume, resampling to a 3 × 3 × 3 mm voxel size using trilinear interpolation. Images were then smoothed with an 8-mm full-width half-maximum (FWHM) Gaussian filter to ameliorate differences in intersubject localization. Data were analyzed using the general linear model approach. At the individual subject level, each task was modelled as a boxcar function (resting blocks were modeled implicitly), and subsequently convolved with the canonical hemodynamic response function. Data were further treated with a high-pass filter with a cutoff of 128 s. Contrasts were calculated to assess differences in activations between the semantic task (synonym judgment) and the control task (number judgment) and vice versa (SEMANTIC–CONTROL and CONTROL–SEMANTIC) and between each task and the resting blocks (SEMANTIC–REST and CONTROL–REST). The subsequent whole-brain multisubject analysis was carried out using a random effects model with a one-sample *t*-test on the summary statistic. Unless stated otherwise, voxel-wise and cluster-wise significance levels were corrected for family-wise error (FWE) using random field theory, as is implemented in SPM5. A priori ROI analyses were performed, including small volume corrections (SVCs) and analyses using the MarsBar ROI toolbox (Brett et al. 2002). MarsBar analyses included the calculation of a single summary value to represent activation across all voxels within the ROI (mean of the parameter estimates).

ROI Construction for Cross-technique Comparisons

ROIs were defined for the purpose of SVC and for analyses using the MarsBar ROI toolbox (Brett et al. 2002). For the SVC, 2 ROIs were defined on the basis of the hypometabolism map reported in a prior (18F)fluor-2-deoxy-D-glucose positron emission tomography (FDG-PET) study of SD (Nestor et al. 2006). (We are grateful to Peter Nestor for making this mask available to us.) This map provides an estimate of the regions affected, on average, in an SD patient sample and thus defines a suitable a priori ROI within which we can attempt to identify specific ATL subregions that are critical to performance of the semantic task (see Results for more details on the rationale behind using an SVC approach). A binary mask was created from the original statistical SD group image, thresholded at $P = 0.05$, corrected (analyzed using SPM99). The left-hemisphere portion of this mask was used as first ROI, while its mirror image in the right hemisphere defined the second ROI so that equally sized search volumes were used to assess activation in each of the temporal lobes (in the original report by Nestor et al., the proportion of the temporal lobe displaying hypometabolic activity was found to be much greater in the left hemisphere than in the right, reflecting the left > right asymmetric atrophy distribution of the SD patients in that study). The anatomical coverage of these ROIs is illustrated in Figure 1*e*. As described by Nestor et al. (2006), each of these ROIs, in their respective hemisphere, covered the entire temporal pole (Brodmann's area [BA] 38), extending caudally to include all regions except the superior temporal gyrus (STG) up until Talairach coordinate $y \approx -20$ (MNI coordinate $y \approx -21$). (Approximate MNI coordinates were estimated using Matthew Brett's Tal2MNI transform [http://imaging.mrc-cbu.cam.ac.uk/imaging/MniTalairach].) Moving posterior to this, the ROI included the fusiform gyrus and the inferior temporal gyrus (ITG) up to Talairach $y \approx -24$ (MNI $y \approx -25$) and thereafter included the fusiform gyrus alone up to, but not including, BA37 (Talairach $y \approx -38$ and MNI $y \approx -39$). These ROI masks were also trimmed so that their lateral and medial extents did not exceed the boundaries of the automated anatomical labeling (AAL: Tzourio-Mazoyer et al. 2002) temporal lobe mask provided in the Wake Forest University Pickatlas toolbox (Maldjian et al. 2003). This ensured the exclusion of white matter and voxels outside of the temporal lobe from the ROIs.

To allow comparison of blood oxygenation level–dependent (BOLD) activation in each gyrus against the volume loss in SD reported by Galton et al. (2001), we defined 5 ROIs corresponding to the STG, the

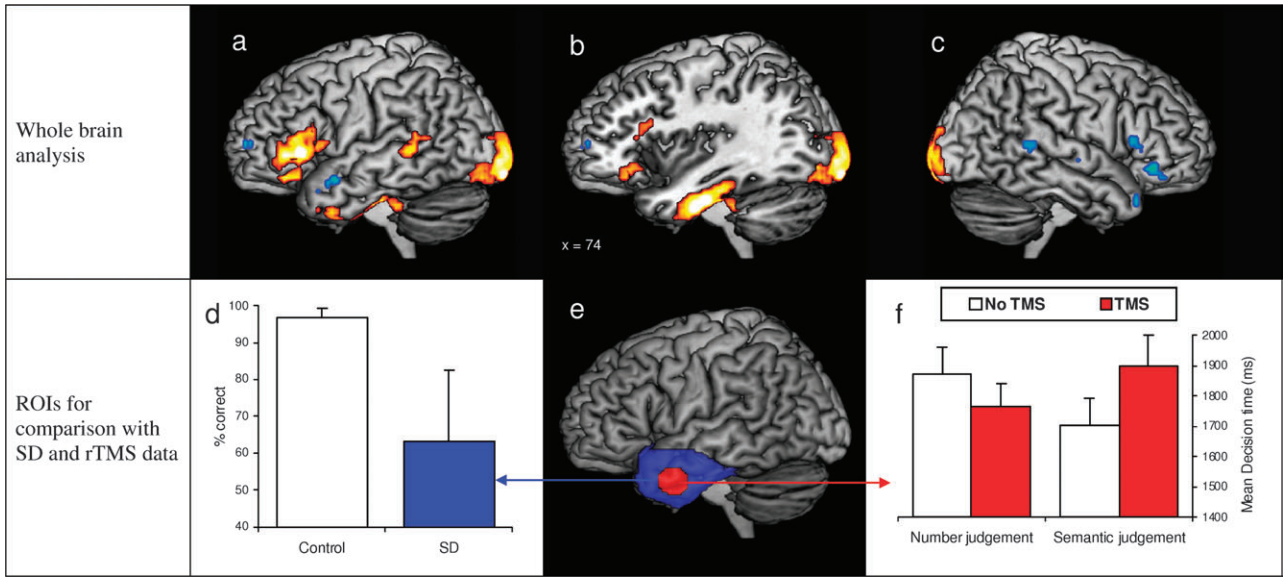

Figure 1. Brain activation maps versus SD and rTMS behavioral data. Brain activation maps show left hemisphere (*a* and *b*) and right hemisphere (*c*) activation in the whole brain analysis of the semantics–numbers contrast. Activations shown in the red/yellow color scale are those surviving cluster-wise $P < 0.05$ FWE-corrected significance thresholding (cluster defining threshold = $P_{uncorrected} < 0.001$; extent threshold = 31 voxels). Additional activations shown in the blue/green color scale are those only surviving voxel-level significance thresholding of $P_{(uncorrected)} < 0.001$. (*d*) Mean accuracy of SD patients performing the semantic task as compared to a healthy age-matched control group. (*e*) ROI derived from a map of hypometabolism in SD patients (blue) and another ROI centred on the mean coordinates of TMS stimulation (red). (*f*) Decision times for the semantic judgement task and the control task both prior to and following 1Hz rTMS over the left ATL.

MTG, the ITG, the fusiform gyrus, and the parahippocampal gyrus of the left hemisphere using the AAL gyral masks in the Pickatlas toolbox. Following the definitions of temporal subvolumes measured by Galton et al., each ROI was trimmed such that their posterior boundaries lay at the coronal slice at which the Sylvian aqueduct is first visible (MNI $y = -26$; slice identified using SPM5's avg152T1 image). In addition, the left-hemisphere hypometabolism ROI was subdivided into the 5-temporal lobe gyri (again using AAL gyral masks in the Pickatlas toolbox), resulting in a further 5 ROIs. Like those just described, these ROIs were used to assess the gyral distribution of BOLD activation but this time specifically within the area that has been shown to be affected in SD on the basis of the hypometabolism study by Nestor et al. (2006). The differences between these 2 sets of ROIs were small however, and there were variations only in the position of the posterior boundaries. This second ROI set covered a smaller proportion of the STG and MTG but a greater proportion of the ITG and the fusiform and parahippocampal gyri (see above).

Finally, to compare BOLD fMRI against the ATL rTMS results, we created a spherical ROI (diameter of 2 cm) centered on the mean stimulation coordinates (in standardized MNI space) for the left (−53, 4, −32) and right (52, 2, −28) ATL sites (Lambon Ralph et al. 2009). As above, each sphere was trimmed with the AAL atlas to exclude extracortical and predominantly white matter voxels.

Results

Whole-Brain Cluster Analyses of Multisubject Contrasts

The data were initially treated to a whole-brain cluster analysis contrasting the semantic task against the numerical control task. The statistical image was assessed for cluster-wise significance using a cluster-defining threshold of $P = 0.001$, and the 0.05 FWE-corrected critical cluster size was 31 voxels (volume = 60 024 voxels; smoothness [FWHM in mm] = 11.5, 11.3, 8.6; RESELS = 1306.2). Table 1 displays the peaks of those clusters that exceeded the critical cluster size. These clusters are also displayed in the red color scale in Figure 1*a–c*, while the activations in the blue color scale are those from the same contrast that only survived an uncorrected voxel-wise threshold of $P < 0.001$. All of these significant clusters were in the left hemisphere. As expected—given the use of the revised imaging protocol (see Introduction and Methods)—we obtained activation in the ATL as well as other cortical regions (commonly activated in standard GE-EPI–based studies). The ATL activation was centered on the left anterior fusiform gyrus but extended rostrally and laterally, terminating on the external surface of the ITG and MTG. This cluster also extended caudally into the most posterior aspects of BA36/BA20 (parahippocampal gyrus and ITG, respectively) and into the anterior lobe of the cerebellum. We also obtained a cluster in the left-hemisphere ventrolateral prefrontal cortex, which included the pars triangularis (BA45), the pars orbitalis (BA47), and possibly also parts of the pars opercularis (BA44). A third activation cluster emerged in the posterior MTG. In addition, there was a large cluster that extended across the left and right occipital lobes (BA17/18)—perhaps reflecting greater visual processing required for orthographic over digit stimuli or even semantic feedback to early visual areas (Hon et al. 2009). Interestingly, the application of an uncorrected voxel height threshold of $P < 0.001$ (with no extent thresholding) revealed a distribution of activated voxels in right hemisphere that closely mirrored the pars triangularis, pars orbitalis, posterior MTG, and temporal pole activation in the left hemisphere (see in the blue color scale in Fig. 1*c*).

The activation maps obtained by contrasting the semantic task against the implicitly modeled "resting" state were also assessed. Analysis used a cluster-defining threshold of $P = 0.001$ and a critical cluster extent threshold of 32 ($P = 0.045$, FWE-corrected, smoothness [FWHM in mm] = 11.2, 11.3, 9.0; RESELS = 1271.1). The results are displayed in Supplementary Figure 1*a,b* and Supplementary Table 1. Temporal lobe activation was largely restricted to clusters in the left hemisphere and largely similar to that revealed when the semantic task was contrasted with numerical judgments (see Supplementary Fig. 1*a,e*). These

Table 1
Significant activation clusters ($P < 0.05$, FWE-corrected) revealed by the contrast of semantic over numerical task

Activation cluster	Cluster extent (voxels)	Maximum *z* value	Peak MNI coordinates		
			x	*y*	*z*
Left fusiform gyrus (plus inferolateral ATL)	217	5.49	−36	−15	−30
Left inferior prefrontal cortex	212	5.27	−54	24	3
Left posterior middle temporal gyrus	77	4.17	−66	−42	3
Bilateral occipital lobe	813	5.56	15	−87	−6

included a cluster in the ventral ATL (peaking in the anterior fusiform gyrus) and another cluster in the anterior STG/superior temporal sulcus (STS). The posterior MTG was once again activated as part of a cluster that originated in the peri-Sylvian postcentral gyrus and arced in a posterior manner across the posterior Sylvian fissure into the posterior temporal lobe. In an extensive network of frontal activation, ventrolateral prefrontal cortex was activated bilaterally, while more dorsal–lateral frontal regions were additionally activated in the right hemisphere. Superior medial frontal gyrus/dorsal anterior cingulate was activated bilaterally. Activations that were not present in the SEMANTICS–NUMBERS contrast were revealed in the left inferior parietal lobule peaking in superior BA40 and in inferior BA40 of the right hemisphere. This can be clearly seen in Supplementary Figure 1 where the activation map from the SEMANTICS–REST contrast (Supplementary Fig. 1*e,f*) is presented alongside that of the SEMANTICS–NUMBERS contrast (Supplementary Fig. 1*a,b*). This figure highlights both the similarities and the differences in the patterns of activation obtained when using a lower- versus a higher-level baseline condition. Another striking difference is the reduced extent of activation in the ventral anterior temporal regions when contrasting the semantic task against a resting baseline. This is such that it no longer includes activation of the more inferolateral aspects of the ATL, which is consistent with the idea that there may be a greater degree of semantic processing (e.g., daydreaming) occurring during the resting condition that reduces the sensitivity of the SEMANTIC–REST contrast for detecting the semantic network (Binder et al. 1999, 2009; Visser et al. forthcoming).

Contrasting the numerical task against the semantic task (NUMBERS–SEMANTICS) found activation in the left precuneus only (MNI coordinates = –6, –72, 42; maximum *z* value = 5.73; voxel height threshold was $P = 0.001$; cluster extent = 111 voxels; cluster-level significance was $P < 0.001$, FWE-corrected). The contrast of the numerical task against rest (cluster-defining threshold of $P = 0.001$; extent threshold = 35; 0.05 FWE-corrected, smoothness [FWHM in mm] = 11.7, 12.0, 9.3; RESELS = 1116.7) revealed activation in the right dorsal–lateral prefrontal cortex and medial superior frontal gyrus and dorsal anterior cingulate, bilaterally. There was an extensive bilateral parietal activation extending both laterally over the angular gyrus (and the left intraparietal sulcus) and medially into the precunei (similar to that found in the SEMANTICS–REST contrast; Supplementary Fig. 1*a,b*). The peaks of this activation were located in BA7 in the left hemisphere and in white matter near to BA39 in the right hemisphere. The results of this contrast are displayed in Supplementary Figure 1*c,d*, and Supplementary Table 2.

Direct Comparison of fMRI, SD, and rTMS

As noted above, as well as using the new fMRI protocol for improving detection of ATL activation, we also adopted the same tasks as those used to assess semantic performance in SD and in our previous ATL rTMS studies (Pobric et al. 2007; Jefferies et al. 2009; Lambon Ralph et al. 2009). This licensed, for the first time, direct neuroanatomical comparisons across the 3 techniques without variation in task or stimuli characteristics (see Introduction). To achieve these direct comparisons, we conducted 2 ROI-based analyses using the contrast of SEMANTICS–NUMBERS, with the a priori ROIs constructed on the basis of neuroanatomical hypotheses drawn from previous investigations of SD and from the rTMS studies (see Methods).

fMRI versus SD

Jefferies et al. (2009) compared the performance of SD patients on the semantic judgment task with that of healthy age-matched controls and, consistent with the wealth of previous semantic testing in this patient group (see Introduction), found them to perform substantially more poorly on this comprehension test (the results are summarized in Fig. 1*d*). The root of this impairment is associated with progressive atrophy of the ATLs bilaterally, with the most extensive damage located in the temporal poles and the inferior and lateral surfaces. FDG–PET studies have shown hypometabolism not only in these specific areas but also across much of the ATL region (Nestor et al. 2006; Desgranges et al. 2007).

In our first 2 ROI analyses, therefore, we examined whether there were any discrete areas within this broader affected region that are active in healthy individuals performing the semantic judgment task. We used the map of glucose hypometabolism reported by Nestor et al. (2006) to define 2 ATL ROIs, 1 in the left hemisphere and 1 in the right. The anatomical coverage of these ROIs is illustrated in Figure 1*e*. We adopted an SVC approach to constrain the correction for multiple comparisons in order to increase the sensitivity of the analysis and control for type 2 errors. This was particularly important, given that inferences were to be made at the voxel level in order to increase "localizing power" (Friston et al. 1996) to detect distinct activation foci. Inferences at the voxel level are particularly vulnerable to type 2 errors when corrections for multiple comparisons are made across large search volumes. Control for type 1 errors was maintained by the use of an FWE-corrected voxel-level significance threshold of $P = 0.05$. The voxels surviving thresholding in the left-hemisphere SVC analysis are listed in Table 2 with their FWE-corrected significance level (volume = 1360 voxels; RESELS = 25.2). Distinct activations were identified at voxels within the middle (MNI coordinates = –36, –15, –30), posterior (–39, –24, –24), and the anterior (–39, –9, –36) aspects of the fusiform cluster found in the whole-brain analysis (all Ps < 0.01, FWE-corrected). Moreover, activation was found at a voxel that had formed the most anterolateral aspect of this cluster in the anterior ITG (–51, 6, –39; $P = 0.067$, FWE-corrected). Most

notably, additional activation was now identified ($P < 0.05$, FWE-corrected) in the anterior STG/STS (–57, 6, –18; for an anatomical reference, see the blue activation in Fig. 1*a*). This area has previously been identified when participants passively listen to meaningful sentences (e.g., Scott et al. 2000; Crinion et al. 2003). The right-hemisphere SVC analysis (volume = 1394 voxels; RESELS = 25) revealed activation that approached significance (voxel z value = 3.80; $P = 0.10$, FWE-corrected) in the very tip of the right temporal pole (45, 24, –33; for an anatomical reference, see in blue in Fig. 1*c*).

The second step made neuroanatomically guided comparisons of the fMRI and SD. Specifically, we compared the relative degree of ATL activations observed in the healthy subjects against the gyral distribution of volume loss measured previously in SD. To achieve this aim, the rostral half of the left temporal lobe (anterior to MNI $y = –26$) was subdivided into 5 separate ROIs, each one corresponding to one of the anterior temporal gyri, forming a set that resembled the subvolumes measured in a magnetic resonance imaging volumetric assessment of tissue loss in subregions of the temporal lobes of 18 SD patients (Galton et al. 2001; see Methods for details). Similarly, we divided the left hypometabolism mask into 5 ROIs corresponding to each of the constituent gyri (see Methods). This licensed an additional analysis contained within the region shown to be affected in SD on the basis of a hypometabolism study (Nestor et al. 2006). In each of these 2 analyses, the relative activation of semantics over number tasks was compared in each gyrus (see Fig. 2*a*) using the MarsBar ROI toolbox (Brett et al. 2002). The 2 sets of results were statistically identical as can be seen in Table 3. We compared these findings with the results of Galton et al. (2001). The average percentage of tissue loss for each gyrus is presented in Figure 2*d* alongside the results of the gyral ROI analysis performed within the borders of the hypometabolism mask (Fig. 2*c*). The parallel between the distribution of BOLD activation in normal participants and the tissue loss in SD is striking. In particular, these values were maximal for the fusiform gyrus (42.5% tissue loss in SD) and the ITG (36.3% loss of ITG/MTG [Galton et al. combined the measures for MTG/ITG in their study] in SD), and these were the only 2 gyri that showed significantly greater activation for semantic over number judgment tasks (fusiform [$P < 0.00001$, Bonferroni correction] and ITG [$P < 0.001$, Bonferroni correction]). This would suggest that the integrity of the anterior ITG and anterior fusiform gyrus is crucial for successful performance of this semantic task (see Discussion).

fMRI versus TMS

Our final ROI analysis focused on the comparison between these fMRI results and the previous rTMS studies (Pobric et al. 2007; Lambon Ralph et al. 2009). The previous rTMS behavioral results for this site (timed synonym vs. number decisions) are summarized in Figure 1*f*, showing the relative slowing for the synonym but not for the number task following left ATL

Table 2
Voxel-wise activations revealed by the small volume correction on the contrast of semantic over numerical task

Brain region	Voxel z value	FWE-corrected P value	MNI coordinates		
			x	y	z
Middle left fusiform gyrus	5.49	<0.0001	−36	−15	−30
Anterior left fusiform gyrus	5.31	<0.0001	−39	−9	−36
Posterior left fusiform gyrus	4.39	0.008	−39	−24	−24
Anterior left superior temporal sulcus	3.97	0.048	−57	6	−18
Anterolateral left inferior temporal gyrus	3.89	0.067	−51	6	−39

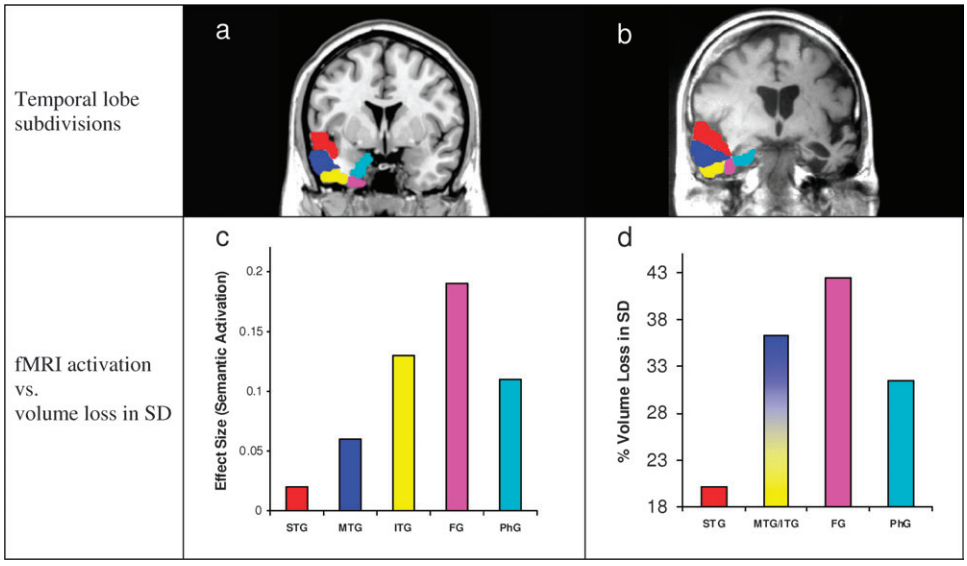

Figure 2. Temporal lobe distribution of semantic activation versus volume loss in SD. (*a*) Temporal lobe gyrus ROIs used to assess the distribution of semantic activation in the ATL. (*b*) Example MR scan of an SD patient overlaid with representations of the temporal lobe ROIs used in a previous volumetric study of SD (Galton et al., 2001). (*c*) Semantic activation (relative to number task) within each of the temporal lobe subdivisions marked in (*a*). (*d*) Distribution of temporal lobe volume loss observed in a group of SD patients.

Table 3
Temporal lobe distribution of semantic activation revealed within 2 independent ROI analyses

	Posterior extents defined according to Galton et al. (2001)			Posterior extents defined according to Nestor et al. (2006)		
	Effect size	*T* value	Bonferroni-corrected *P* value	Effect size	*T* value	Bonferroni-corrected *P* value
STG	−0.02	−0.44	1.00000	0.02	0.21	1.00000
MTG	0.06	1.98	0.17242	0.06	1.9	0.20122
ITG	0.13	5.57	<0.001	0.13	5.51	<0.001
Fusiform gyrus	0.17	8.46	<0.00001	0.19	8.45	<0.00001
Parahippocampal gyrus	0.18	1.48	0.40528	0.11	1.4	0.46394

stimulation. We assessed local activation at the site that had been stimulated (a superior and lateral area overlying the MTG; see Fig. 1*e* and Methods) using the MarsBar toolbox. As expected from the rTMS studies, the analysis revealed that this left-hemisphere rTMS ROI was indeed more active for the synonym than for number judgment tasks in this fMRI study ($P < 0.005$, Bonferroni correction). However, while Lambon Ralph et al. (2009) also reported statistically identical slowing for the synonym task following right ATL stimulation, our analysis did not find significant activation within a right TMS ROI.

Discussion

Although not considered in some contemporary reviews of semantic cognition or language (e.g., Mesulam 1998; Catani and ffytche 2005), there is a growing consensus that the ATLs contribute to the formation and activation of semantic knowledge (Patterson et al. 2007; Lambon Ralph and Patterson 2008; Simmons and Martin 2009). This is based on a growing body of evidence derived from neuropsychology (in particular SD), MEG, PET neuroimaging, and rTMS studies of healthy participants (e.g., Vandenberghe et al. 1996; Marinkovic et al. 2003; Wise 2003; Rogers et al. 2006; Spitsyna et al. 2006; Pobric et al. 2007; Lambon Ralph et al. 2009). At present, however, all of this evidence converges somewhat coarsely upon a rather broad area of temporal cortex, and the use of the term "ATL" often refers to the extensive anterior region typically affected in SD (see Introduction). As a consequence, the research focus is now shifting toward 2 subsequent questions: Which specific ATL subregions are most strongly implicated in semantic cognition and what type of knowledge or role does each of them contribute?

This study was concerned with the first of these 2 key questions. It was tackled by utilizing a novel direct comparison of spatially corrected spin-echo fMRI, with rTMS and SD that allowed us to assess commonality between the more precise neuroanatomical hypotheses that can be derived from these 3 methodologies. This approach was licensed by 2 key methodological developments. The first was to make use of the same semantic and control tasks in the fMRI experiment as those used previously in the rTMS and SD studies (Pobric et al. 2007; Jefferies et al. 2009; Lambon Ralph et al. 2009)—thereby removing differences induced by varying the tasks themselves across each source of empirical data (TMS, patients, or imaging). This enabled a uniquely controlled comparison of the neuroanatomical hypotheses drawn from 3 independent modalities. The second aspect concerned previous limitations imposed by the fact that conventional GE-EPI fMRI is vulnerable to signal loss and distortion. This is caused by variation in magnetic susceptibility, which is particularly pronounced within polar and ventral temporal and orbitofrontal areas (Dong et al. 2005; Blacker et al. 2006; Weiskopf et al. 2006). Although not a problem for other neuroimaging techniques such as PET and MEG (Devlin et al. 2000; Marinkovic et al. 2003), these methods have other practical limitations that make fMRI preferable for pursuing our primary objective. In the current study, therefore, we made use of recent fMRI developments that substantially reduce the problems associated with obtaining signal from the ATLs (Embleton et al. forthcoming; Visser et al. in preparation). By using improvements in modern scanners (e.g., parallel receiver coils) as well as an SE-EPI sequence and a spatial correction technique, it is possible to maintain whole-brain coverage with improved sensitivity to ATL signal even for the problematic ventral and polar regions.

The whole-brain analyses revealed 4 core regions when activation for semantic judgments was compared with that for number or rest conditions. As expected from previous neuropsychological and neuroimaging studies of language and semantic cognition, these included the left posterior MTG, left inferior prefrontal cortex, left inferior parietal cortex (iPC) (although only for the comparison against rest), and the left ATL. Within the ATL, there were 2 distinct foci of activation, perhaps suggesting that semantic function within this area is discretely localizable to specific subregions. Moreover, by comparing our fMRI results with those of previous rTMS and SD studies, we were able to demonstrate a tight convergence across the 3 methods with regard to these ATL subregions. These results plus their potential implications are discussed in the following sections.

Left Anterior Ventral and Inferolateral Temporal Lobes

By far, the strongest temporal lobe activation was found on the ventral surface, running along the left fusiform gyrus and then dorsolaterally up onto the lateral surface of the anterior ITG. Furthermore, the SVC approach identified 4 separate peaks within this cluster (see Table 2), the strongest of which was in the anterior third of the fusiform gyrus. Overall, this pattern fits with the results of a volumetric analysis of atrophy in SD (Galton et al. 2001), particularly given that these patients have also been shown to perform substantially more poorly than healthy controls on this same synonym judgment task (Jefferies et al. 2009). The parallel between the gyral distribution of normal semantic activation and volume loss in SD is strikingly similar (see Fig. 2). Both measures peak in the anterior ITG-fusiform gyrus and drop off in the more medial and dorsolateral anterior temporal gyri, providing tight convergent evidence that the left anterior fusiform gyrus is especially important for the processing of verbal semantics. A number of PET-based neuroimaging studies of language function have found activation of the anterior ventral ATL in response to both visually and aurally presented stimuli (Nobre et al. 1994; Noppeney and Price 2002; Crinion et al. 2003; Sharp et al. 2004; Spitsyna et al. 2006). Furthermore, our activation lines up with a ventral area identified in a recent meta-analysis of 120 functional neuroimaging studies of semantic processing (Binder et al. 2009) but it also extends more anteriorly, perhaps due to the signal

recovered by virtue of the distortion correction. This region is frequently referred to as the "basal temporal language area" following the work of Luders et al. (1986, 1991) who demonstrated that direct electrical stimulation of the anterior fusiform gyrus elicits selective language interference with a predominantly receptive nature. Burnstine et al. (1990) found that this was also true of stimulation to the anterior portions of the ITG and the parahippocampal gyrus. Its function does not seem to be specific to language processes, however. This area is also highlighted within models of higher visual processing (e.g., Felleman and Van Essen 1991; Rolls 1991; Deco and Rolls 2004), which describe a hierarchy of processing stages that proceed anteriorly along the ventral temporal lobe, with representations becoming increasingly complex and invariant, ultimately developing into supramodal associations around the point of the ventral ATL (also see Halgren et al. 2006). Consistent with this, a recent human intracranial electrode potential study found that cells in this anterior ventral region respond extremely rapidly to nonverbal visual stimuli and in a highly invariant and semantically specific fashion (Liu et al. 2009). There are various parallel but unrelated lines of research that appear to be converging on the hypothesis that the information encoded within the anterior ventral temporal lobe is amodal and also that activity in this area is closely related to semantic processes. For example, studies examining presurgical intracortical electrode recordings and event-related MEG responses have found both auditory and visual responses in this area that appear to be related to semantic manipulations (N400; Marinkovic et al. 2003; Halgren et al. 2006). While other areas may also make critical contributions, these convergent results lead us to speculate that this anatomical region is a core substrate for the amodal "semantic hub" postulated in contemporary theories of semantic memory (Rogers et al. 2004; Patterson et al. 2007; Lambon Ralph and Patterson 2008; Lambon Ralph et al. forthcoming).

Anterior MTG/STS

Semantic activation was also revealed in a more lateral anterior MTG/STS region. Our previous work has shown that low-frequency rTMS targeting this very area results in a slowing of performance on the synonym judgment task (Pobric et al. 2007; Lambon Ralph et al. 2009). Together, these findings provide compelling evidence for a role of this more superior and lateral region in semantic processing, although its precise function remains elusive. One frequent speculation is that it may be involved in sentence-level semantic or syntactic processing of speech (see Hickok and Poeppel 2004). This suggestion does not seem to fit with the presentation of SD patients or the results from the current study. Specifically, despite sometimes severe semantic impairment, SD patients have excellent receptive and expressive syntax (Schwartz et al. 1979; Hodges et al. 1992). In addition, the synonym task used in this study was based on single concepts and not sentences. The same is true of other semantic tasks (e.g., Devlin et al. 2000). As for the ventral temporal lobe, there is evidence to suggest that processing of auditory stimuli occurs in hierarchically organized fashion along the STG, with the complexity of preferred stimuli and the perceptual invariance of responses increasing toward the temporal pole (see Rauschecker and Scott 2009). The anterior MTG/STS would appear to reside at the very end of this auditory "what" pathway. It has been noted in numerous other functional neuroimaging studies and appears to respond as a function of meaningfulness as opposed to stimulus complexity alone (Scott et al. 2000; Crinion et al. 2003; Rauschecker and Scott 2009). In addition, functional data from the nonhuman primate cortex indicate that the STS is responsive to visual, auditory, and somatosensory stimuli, and therefore, it has been regarded as polysensory association cortex (Bruce et al. 1981; Poremba et al. 2003). Similar conclusions can be drawn from primate connectivity data (Seltzer and Pandya 1978). Overall therefore, with regard to a functional role of the anterior MTG/STS in semantic cognition, we might consider 2 alternative possibilities that require further empirical exploration: 1) it may constitute an additional amodal representational "hub" or 2) it may provide an interface between highly processed auditory input and more inferiorly located amodal semantic representations.

Further Consideration of the Potential Functional Specialization within the ATL

Our results suggest that there are 2 specific ATL subregions that are particularly important to the performance of a semantic task. The failure to reject the null hypothesis within other ATL subregions, however, does not necessarily preclude the possibility that they also have a role in semantic processing. It is useful, therefore, to briefly consider some of the potential hypotheses regarding the function of these other subregions. First, it is possible that this study has merely identified the peaks of activation, or functional epicenters, of a distributed semantic processing system located within the ATL. In this case, it might be that activation in other ATL subregions only becomes detectable when the complexities of the semantic computations required by a task are significantly increased, and there are greater demands on processing resources. Alternatively, given that our task was presented in the verbal domain, it is possible that we have identified the ATL subregions that are relatively more specialized for processing verbal semantics. Other ATL subregions may be more responsive to nonverbal stimuli. Another possibility is that their function relates to other pre- or postsemantic processes. For example, it has been suggested that the temporal pole (corresponding approximately to BA38) has a role in binding highly processed perceptual information with emotional responses located in the limbic cortex (Olson et al. 2007; Ross and Olson 2010). Clearly though, further work is required to elucidate upon the potential of each of these hypotheses.

Lateralization of ATL Semantic Function

The semantic activation observed in this fMRI study was strongly lateralized to the left hemisphere. The SVC did, however, reveal activation approaching significance in the very rostral tip of the right temporal lobe. This would suggest that the right ATL was in fact active but that its response to the task was by far weaker and less extensive than that of the left ATL. This is of particular interest because SD always arises in the context of bilateral ATL atrophy/hypometabolism, although it is often asymmetrically distributed. Furthermore, Lambon Ralph et al. (2009) have demonstrated that rTMS over the left versus the right ATL produces equivalent slowing of performance in the synonym judgment task. Taken together, the SD and rTMS results suggest that the ATL semantic system is effectively bilateral (Lambon Ralph et al. 2009), but the results

of the present study do not seem to be perfectly consistent with this. One possible interpretation of the apparent lateralization of activation is that it reflects the importance of language processing in this particular semantic task. This is consistent with the observation that SD patients with more left than right ATL atrophy have a more pronounced naming deficit than those with the opposite atrophic distribution (right > left) (Lambon Ralph et al. 2001). In attempting to explain this, the authors proposed that the left ATL is more actively engaged in tasks that include a strong verbal component because of its closer proximity and more extensive connections to the left-lateralized dominant language centers. It might also be the case that the right ATL is preferentially connected to networks that are predominately right lateralized (e.g., face processing; see Snowden et al. 2004). The results of our previous rTMS study (Lambon Ralph et al. 2009) would appear, however, to rule out an absolute division of labor across the 2 ATLs in terms of task modality. Our understanding of the way in which the left and right ATLs contribute to semantic memory will be enhanced by further rTMS and neuroimaging studies designed specifically to tackle this issue.

Non-ATL Semantic Areas

Theories advocating a role for the ATL in semantic cognition (semantically driven behavior) do not assume that it is the only brain region involved (Patterson et al. 2007; Lambon Ralph and Patterson 2008). Instead, it is clear from this and many other patient and neuroimaging studies that semantic cognition is supported by a network of brain areas, including left ventrolateral prefrontal cortex (vlPFC), left posterior temporal cortex, the left temporoparietal junction, inferior parietal cortex (iPC), and the ATL. Broadly speaking, these can be split into 2 types: information-bearing regions and control/regulatory areas. For example, following models of cognitive control (Garavan et al. 2000; Peers et al. 2005), there is now fMRI, rTMS, and patient evidence to suggest that anterior vlPFC helps to shape or in some way regulate which aspects of meaning are relevant to the language or nonverbal activity in hand (Thompson-Schill et al. 1997; Wagner et al. 2001; Devlin et al. 2003; Jefferies and Lambon Ralph 2006; Jefferies et al. 2007). Therefore, this region would be especially important when complex semantic judgments are needed, when there is strong intrinsic competition between alternative meanings and in everyday verbal and nonverbal activities that require some but not all aspects of the meaning. The vlPFC activation observed in the current study spanned both the pars orbitalis and the pars triangularis. Attempts have been made to dissociate the relative contributions of these 2 regions to control processes, and it has been suggested that the pars orbitalis may be more specifically involved in semantic selection/retrieval; posterior vlPFC (pars opercularis) is more involved in phonological processes, while mid-vlPFC (pars triangularis) appears to play a role in more general postretrieval selection processes (Poldrack et al. 1999; Devlin et al. 2003; Dobbins and Wagner 2005; Gough et al. 2005). Although the design of the current study is such that we cannot confidently comment on the specific contribution of these 3 areas, the data are consistent with the idea that at least the pars triangularis and the pars orbitalis belong to a network involved in semantic cognition. However, the fact that these areas were not activated by the control task would suggest that these purported roles are not generalizable to the numerical domain.

iPC has been implicated in both verbal response and semantic selection (Thompson-Schill et al. 1997; Schumacher et al. 2003). Its activity has been shown to increase with difficulty in both types of selection, leading to the speculation that neurally distinct prefrontal regions may put response and semantic control processes into effect by modulating common posterior regions, such as the iPC (Nagel et al. 2008). Our data are consistent with this hypothesis; the iPC was active when participants made semantic judgments and when they made numerical magnitude judgments. In contrast, while some prefrontal regions were activated in both tasks (right dorsolateral PFC), activation of the ventrolateral prefrontal cortex occurred only during the semantic task (see Supplementary Fig. 1).

The Importance of the Appropriate Choice of Baseline Task

The importance of choosing appropriate baseline tasks for detecting the semantic network via subtractive analyses has been highlighted in previous meta-analyses and empirical investigations (e.g., Binder et al. 1999, 2009; Visser et al. forthcoming). We have shown that contrasting activation elicited by a semantic task against activation during a high-level active baseline demonstrates increased sensitivity to ATL activation as compared with contrasts against low-level resting state conditions, thereby reemphasising the importance of such methodological decisions for future studies of ATL semantic function.

Summary

To conclude, in addition to various prefrontal and posterior temporoparietal regions, there is growing evidence for the involvement of the ATL in semantic cognition. There is much, however, to be understood regarding which aspects of this region are important and their precise contribution. In a novel attempt to elucidate, the current study compared novel functional neuroimaging data with a neuropsychological study of SD and rTMS studies of healthy individuals that had employed an identical task and stimuli set. Together, these studies highlight the anterior ventral and inferolateral temporal lobe and the anterior MTG/STS as critical for normal performance of the semantic computations required by the task and thereby impose new constraints upon neuroanatomical hypotheses regarding ATL involvement in semantic memory.

Funding

Medical Research Council (MRC) program grant (G0501632) and MRC Pathfinder grant (G0300952).

Supplementary Material

Supplementary material can be found at: http://www.cercor.oxfordjournals.org/

Notes

Conflict of Interest: None declared.

References

Binder JR, Desai RH, Graves WW, Conant LL. 2009. Where is the semantic system? A critical review and meta-analysis of 120 functional neuroimaging studies. Cereb Cortex. 19:2767–2796.

Binder JR, Frost JA, Hammeke TA, Bellgowan PSF, Rao SM, Cox RW. 1999. Conceptual processing during the conscious resting state: a functional MRI study. J Cogn Neurosci. 11:80–93.
Blacker D, Byrnes ML, Mastaglia FL, Thickbroom GW. 2006. Differential activation of frontal lobe areas by lexical and semantic language tasks: a functional magnetic resonance imaging study. J Clin Neurosci. 13:91–95.
Bozeat S, Lambon Ralph MA, Graham KS, Patterson K, Wilkin H, Rowland J, Rogers TT, Hodges JR. 2003. A duck with four legs: investigating the structure of conceptual knowledge using picture drawing in semantic dementia. Cogn Neuropsychol. 20:27–47.
Bozeat S, Lambon Ralph MA, Patterson K, Garrard P, Hodges JR. 2000. Non-verbal semantic impairment in semantic dementia. Neuropsychologia. 38:1207–1215.
Bozeat S, Lambon Ralph MA, Patterson K, Hodges J. 2002. When objects lose their meaning: what happens to their use? Cogn Affect Behav Neurosci. 2:236–251.
Brett M, Anton JL, Valbregue R, Poline JB. 2002. Region of interest analysis using an SPM toolbox [abstract]. In: 8th International Conference on Functional Mapping of the Human Brain, June 2–6, Sendai, Japan. Available on CD-ROM in NeuroImage. 16.
Brodmann K. 1909. Vergleichende lokalisationslehre der Grosshirnrinde. Leipzig (Germany): Barth.
Bruce C, Desimone R, Gross CG. 1981. Visual properties of neurons in a polysensory area in superior temporal sulcus of the macaque. J Neurophysiol. 46:369–384.
Burnstine TH, Lesser RP, Hart J, Uematsu S, Zinreich SJ, Krauss GL, Fisher RS, Vining EPG, Gordon B. 1990. Characterization of the basal temporal language area in patients with left temporal-lobe epilepsy. Neurology. 40:966–970.
Catani M, ffytche DH. 2005. The rises and falls of disconnection syndromes. Brain. 128:2224–2239.
Chan D, Fox NC, Scahill RI, Crum WR, Whitwell JL, Leschziner G, Rossor AM, Stevens JM, Cipolotti L, Rossor MN. 2001. Patterns of temporal lobe atrophy in semantic dementia and Alzheimer's disease. Ann Neurol. 49:433–442.
Coccia M, Bartolini M, Luzzi S, Provinciali L, Lambon Ralph M. 2004. Semantic memory is an amodal, dynamic system: evidence from the interaction of naming and object use in semantic dementia. Cogn Neuropsychol. 21:513–527.
Crinion JT, Lambon-Ralph MA, Warburton EA, Howard D, Wise RJS. 2003. Temporal lobe regions engaged during normal speech comprehension. Brain. 126:1193–1201.
Deco G, Rolls ET. 2004. A neurodynamical cortical model of visual attention and invariant object recognition. Vision Res. 44:621–642.
Desgranges B, Matuszewski V, Piolino P, Chetelat G, Mezenge F, Landeau B, De la Sayette V, Belliard S, Eustache F. 2007. Anatomical and functional alterations in semantic dementia: a voxel-based MRI and PET study. Neurobiol Aging. 28:1904–1913.
Devlin JT, Matthews PM, Rushworth MFS. 2003. Semantic processing in the left inferior prefrontal cortex: a combined functional magnetic resonance imaging and transcranial magnetic stimulation study. J Cogn Neurosci. 15:71–84.
Devlin JT, Russell RP, Davis MH, Price CJ, Wilson J, Moss HE, Matthews PM, Tyler LK. 2000. Susceptibility-induced loss of signal: comparing PET and fMRI on a semantic task. NeuroImage. 11:589–600.
Ding S, Van Hoesen GW, Cassell MD, Poremba A. 2009. Parcellation of human temporal polar cortex: a combined analysis of multiple cytoarchitectonic, chemoarchitectonic, and pathological markers. J Comp Neurol. 514:595–623.
Dobbins IG, Wagner AD. 2005. Domain-general and domain-sensitive prefrontal mechanisms for recollecting events and detecting novelty. Cereb Cortex. 15:1768–1778.
Dong Y, Nakamura K, Okada T, Hanakawa T, Fukuyama H, Mazziotta JC, Shibasaki H. 2005. Neural mechanisms underlying the processing of Chinese words: an fMRI study. Neurosci Res. 52:139–145.
Embleton KV, Haroon HA, Morris DM, Lambon Ralph MA, Parker GJM. Forthcoming. Distortion correction for diffusion weighted MRI and tractography in the temporal lobes. Human Brain Mapp.
Felleman DJ, Van Essen DC. 1991. Distributed hierarchical processing in the primate cerebral cortex. Cereb Cortex. 1:1–47.
Fernandez E, Alfaro A, Tormos JM, Climent R, Martinez M, Vilanova H, Walsh V, Pascual-Leone A. 2002. Mapping of the human visual cortex using image-guided transcranial magnetic stimulation. Brain Res Protoc. 10:115–124.
Friston KJ, Holmes A, Poline JB, Price CJ, Frith CD. 1996. Detecting activations in PET and fMRI: levels of inference and power. NeuroImage. 4:223–235.
Galton CJ, Patterson K, Graham K, Lambon-Ralph MA, Williams G, Antoun N, Sahakian BJ, Hodges JR. 2001. Differing patterns of temporal atrophy in Alzheimer's disease and semantic dementia. Neurology. 57:216–225.
Garavan H, Ross TJ, Li SJ, Stein EA. 2000. A parametric manipulation of central executive functioning. Cereb Cortex. 10:585–592.
Gloor P. 1997. The temporal lobe and the limbic system. Oxford: Oxford University Press.
Gough PM, Nobre AC, Devlin JT. 2005. Dissociating linguistic processes in the left inferior frontal cortex with transcranial magnetic stimulation. J Neurosci. 25:8010–8016.
Halgren E, Wang CM, Schomer DL, Knake S, Marinkovic K, Wu JL, Ulbert I. 2006. Processing stages underlying word recognition in the anteroventral temporal lobe. NeuroImage. 30:1401–1413.
Hamdy S, Aziz Q, Rothwell JC, Singh KD, Barlow J, Hughes DG, Tallis RC, Thompson DG. 1996. The cortical topography of human swallowing musculature in health and disease. Nat Med. 2:1217–1224.
Hickok G, Poeppel D. 2004. Dorsal and ventral streams: a framework for understanding aspects of the functional anatomy of language. Cognition. 92:67–99.
Hodges JR, Patterson K, Oxbury S, Funnell E. 1992. Semantic dementia: progressive fluent aphasia with temporal lobe atrophy. Brain. 115:1783–1806.
Hon N, Thompson R, Sigala N, Duncan J. 2009. Evidence for long-range feedback in target detection: detection of semantic targets modulates activity in early visual areas. Neuropsychologia. 47:1721–1727.
Jefferies E, Baker SS, Doran M, Lambon Ralph MA. 2007. Refractory effects in stroke aphasia: a consequence of poor semantic control. Neuropsychologia. 45:1065–1079.
Jefferies E, Lambon Ralph MA. 2006. Semantic impairment in stroke aphasia versus semantic dementia: a case-series comparison. Brain. 129:2132–2147.
Jefferies E, Patterson K, Jones RW, Lambon Ralph MA. 2009. Comprehension of concrete and abstract words in semantic dementia. Neuropsychology. 23:492–499.
Krings T, Naujokat C, Von Keyserlingk DG. 1998. Representation of cortical motor function as revealed by stereotactic transcranial magnetic stimulation. Electroencephalogr Clin Neurophysiol. 109:85–93.
Lambon Ralph MA, Graham KS, Patterson K, Hodges JR. 1999. Is a picture worth a thousand words? Evidence from concept definitions by patients with semantic dementia. Brain Lang. 70:309–335.
Lambon Ralph MA, McClelland JL, Patterson K, Galton CJ, Hodges JR. 2001. No right to speak? The relationship between object naming and semantic impairment: neuropsychological evidence and a computational model. J Cogn Neurosci. 13:341–356.
Lambon Ralph MA, Patterson K. 2008. Generalization and differentiation in semantic memory. Ann N Y Acad Sci. 1124:61–76.
Lambon Ralph MA, Pobric G, Jefferies E. 2009. Conceptual knowledge is underpinned by the temporal pole bilaterally: convergent evidence from rTMS. Cereb Cortex. 19:832–838.
Lambon Ralph MA, Sage K, Jones RW, Mayberry EJ. Forthcoming. Coherent concepts are computed in the anterior temporal lobes. Proc Natl Acad Sci U S A.
Levy WJ, Amassian VE, Schmid UD, Jungreis C. 1991. Mapping of motor cortex gyral sites non-invasively by transcranial magnetic stimulation in normal subjects and patients. Electroencephalogr Clin Neurophysiol Suppl. 43:51–75.
Liu HS, Agam Y, Madsen JR, Kreiman G. 2009. Timing, timing, timing: fast decoding of object information from intracranial field potentials in human visual cortex. Neuron. 62:281–290.
Luders H, Lesser RP, Hahn J, Dinner DS, Morris H, Resor S, Harrison M. 1986. Basal temporal language area demonstrated by electrical-stimulation. Neurology. 36:505–510.

Luders H, Lesser RP, Hahn J, Dinner DS, Morris HH, Wyllie E, Godoy J. 1991. Basal temporal language area. Brain. 114:743–754.
Luzzi S, Snowden JS, Neary D, Coccia M, Provinciali L, Lambon Ralph MA. 2007. Distinct patterns of olfactory impairment in Alzheimer's disease, semantic dementia, frontotemporal dementia, and corticobasal degeneration. Neuropsychologia. 45:1823–1831.
Maldjian JA, Laurienti PJ, Kraft RA, Burdette JH. 2003. An automated method for neuroanatomic and cytoarchitectonic atlas-based interrogation of fMRI data sets. NeuroImage. 19:1233–1239.
Marinkovic K, Dhond RP, Dale AM, Glessner M, Carr V, Halgren E. 2003. Spatiotemporal dynamics of modality-specific and supramodal word processing. Neuron. 38:487–497.
Martin A. 2007. The representation of object concepts in the brain. Annu Rev Psychol. 58:25–45.
Mesulam MM. 1998. From sensation to cognition. Brain. 121:1013–1052.
Morán MA, Mufson EJ, Mesulam MM. 1987. Neural inputs into the temporopolar cortex of the rhesus monkey. J Comp Neurol. 256:88–103.
Morgan PS, Bowtell RW, McIntyre DJO, Worthington BS. 2004. Correction of spatial distortion in EPI due to inhomogeneous static magnetic fields using the reversed gradient method. J Magn Reson Imaging. 19:499–507.
Mummery CJ, Patterson K, Price CJ, Ashburner J, Frackowiak RSJ, Hodges JR. 2000. A voxel-based morphometry study of semantic dementia: relationship between temporal lobe atrophy and semantic memory. Ann Neurol. 47:36–45.
Nagel IE, Schumacher EH, Goebel R, D'Esposito M. 2008. Functional MRI investigation of verbal selection mechanisms in lateral prefrontal cortex. NeuroImage. 43:801–807.
Nestor PJ, Fryer TD, Hodges JR. 2006. Declarative memory impairments in Alzheimer's disease and semantic dementia. NeuroImage. 30:1010–1020.
Nobre AC, Allison T, McCarthy G. 1994. Word recognition in the human inferior temporal-lobe. Nature. 372:260–263.
Noppeney U, Price CJ. 2002. A PET study of stimulus- and task-induced semantic processing. NeuroImage. 15:927–935.
Oldfield RC. 1971. The assessment and analysis of handedness: the Edinburgh inventory. Neuropsychologia. 9:97–113.
Olson IR, Plotzker A, Ezzyat Y. 2007. The Enigmatic temporal pole: a review of findings on social and emotional processing. Brain. 130:1718–1731.
Patterson K, Nestor PJ, Rogers TT. 2007. Where do you know what you know? The representation of semantic knowledge in the human brain. Nat Rev Neurosci. 8:976–987.
Peers PV, Ludwig CJH, Rorden C, Cusack R, Bonfiglioli C, Bundesen C, Driver J, Antoun N, Duncan J. 2005. Attentional functions of parietal and frontal cortex. Cereb Cortex. 15:1469–1484.
Piwnica-Worms KE, Omar R, Hailstone JC, Warren JD. Forthcoming. Flavour processing in semantic dementia. Cortex.
Pobric G, Jefferies E, Ralph MAL. 2007. Anterior temporal lobes mediate semantic representation: mimicking semantic dementia by using rTMS in normal participants. Proc Natl Acad Sci U S A. 104:20137–20141.
Poldrack RA, Wagner AD, Prull MW, Desmond JE, Glover GH, Gabrieli JDE. 1999. Functional specialization for semantic and phonological processing in the left inferior prefrontal cortex. NeuroImage. 10:15–35.
Poremba A, Saunders RC, Crane AM, Cook M, Sokoloff L, Mishkin M. 2003. Functional mapping of the primate auditory system. Science. 299:568–572.
Rauschecker JP, Scott SK. 2009. Maps and streams in the auditory cortex: nonhuman primates illuminate human speech processing. Nat Neurosci. 12:718–724.
Rogers TT, Hocking J, Noppeney U, Mechelli A, Gorno-Tempini ML, Patterson K, Price CJ. 2006. Anterior temporal cortex and semantic memory: reconciling findings from neuropsychology and functional imaging. Cogn Affect Behav Neurosci. 6:201–213.
Rogers TT, Lambon Ralph MA, Garrard P, Bozeat S, McClelland JL, Hodges JR, Patterson K. 2004. Structure and deterioration of semantic memory: a neuropsychological and computational investigation. Psychol Rev. 111:205–235.
Rogers TT, McClelland JL. 2004. Semantic cognition: a parallel distributed processing approach. Cambridge (MA): MIT Press.
Rolls ET. 1991. Neural organization of higher visual functions. Curr Opin Neurobiol. 1:274–278.
Ross LA, Olson IR. 2010. Social cognition and the anterior temporal lobes. NeuroImage. 49:3452–3402.
Schumacher EH, Elston PA, D'Esposito M. 2003. Neural evidence for representation-specific response selection. J Cogn Neurosci. 15:1111–1121.
Schwartz MF, Marin OSM, Saffran EM. 1979. Dissociations of language function in dementia: a case study. Brain Lang. 7:277–306.
Scott SK, Blank CC, Rosen S, Wise RJS. 2000. Identification of a pathway for intelligible speech in the left temporal lobe. Brain. 123: 2400–2406.
Seltzer B, Pandya DN. 1978. Afferent cortical connections and architectonics of superior temporal sulcus and surrounding cortex in rhesus-monkey. Brain Res. 149:1–24.
Sharp DJ, Scott SK, Wise RJS. 2004. Retrieving meaning after temporal lobe infarction: the role of the basal language area. Ann Neurol. 56:836–846.
Simmons WK, Martin A. 2009. The anterior temporal lobes and the functional architecture of semantic memory. J Int Neuropsychol Soc. 15:645–649.
Snowden JS, Thompson JC, Neary D. 2004. Knowledge of famous faces and names in semantic dementia. Brain. 127:860–872.
Spitsyna G, Warren JE, Scott SK, Turkheimer FE, Wise RJS. 2006. Converging language streams in the human temporal lobe. J Neurosci. 26:7328–7336.
Studholme C, Cardenas V, Blumenfeld R, Schuff N, Rosen HJ, Miller B, Weiner M. 2004. Deformation tensor morphometry of semantic dementia with quantitative validation. NeuroImage. 21:1387–1398.
Thompson-Schill SL, D'Esposito M, Aguirre GK, Farah MJ. 1997. Role of left inferior prefrontal cortex in retrieval of semantic knowledge: a reevaluation. Proc Natl Acad Sci U S A. 94:14792–14797.
Tzourio-Mazoyer N, Landeau B, Papathanassiou D, Crivello F, Etard O, Delcroix N, Mazoyer B, Joliot M. 2002. Automated anatomical labeling of activations in SPM using a macroscopic anatomical parcellation of the MNI MRI single-subject brain. NeuroImage. 15:273–289.
Vandenberghe R, Price C, Wise R, Josephs O, Frackowiak RSJ. 1996. Functional anatomy of a common semantic system for words and pictures. Nature. 383:254–256.
Visser M, Jefferies E, Lambon Ralph MA. Forthcoming. Semantic processing in the anterior temporal lobes: a meta-analysis of the functional neuroimaging literature. J Cogn Neurosci.
Wagner AD, Paré-Blagoev EJ, Clark J, Poldrack RA. 2001. Recovering meaning: left prefrontal cortex guides controlled semantic retrieval. Neuron. 31:329–338.
Weiskopf N, Hutton C, Josephs O, Deichmann R. 2006. Optimal EPI parameters for reduction of susceptibility-induced BOLD sensitivity losses: a whole-brain analysis at 3 T and 1.5 T. NeuroImage. 33:493–504.
Wise RJS. 2003. Language systems in normal and aphasic human subjects: functional imaging studies and inferences from animal studies. Br Med Bull. 65:95–119.